Journal for Geometry and Graphics
Volume 19 (2015), No. 1, 1–11.

Visualization of Fractals Based on Regular Convex Polychora

Andrzej Katunin

Institute of Fundamentals of Machinery Design, Silesian University of Technology
Konarskiego 18A, 44-100 Gliwice, Poland
email: andrzej.katunin@polsl.pl

Abstract. The paper deals with methods of visualizing deterministic fractals based on regular convex polychora in the four-dimensional (4D) Euclidean space. A survey of different approaches used in the visualization of 4D graphics is presented on examples of fractals using various techniques. The problem of information losses during the projection process from 4D to 3D is analyzed and discussed. It is concluded that there is no single strict rule for the visualization of 4D fractals; the type of projection should be chosen depending on unique geometric characteristics of the given 4D fractal.

Key Words: deterministic fractals, four-dimensional geometry, regular convex polychora, projection of higher-dimensional data

MSC 2010: 51N05, 51M20, 28A80

1. Introduction

A visual representation of objects, even in 3D space, requires an appropriate projection, which always results in a loss of information in the case when only one image is used for such a representation. Depending on the chosen projection type and on geometric characteristics of the projected object, an information loss can be reduced or enlarged. One of the crucial factors during the visualization of higher-dimensional objects is the selection of an appropriate projection and an appropriate observation direction, considering the specific shape characteristics of the depicted object.

An analysis of the visualization of higher-dimensional polytopes was carried out by Séquin [23]. He analyzed the influence of the symmetry of an object and of the type of projection on a pleasant visual impression and the comprehensibility of the projected object. The problem of visual representations of higher-dimensional data and objects was investigated by many authors, who used different approaches. One of the earliest approaches is a wire-frame or skeleton representation of edges of an object [17, 9]. The specific case of such projections is an orthogonal wire-frame projection (the projection of an object to a 2D plane, where many lines of the object are orthogonal to the projection plane) known as *Petrie*

ISSN 1433-8157/$ 2.50

polygon [2]. Another projection type uses a perspective projection from some point outside the object's hypervolume oriented toward a chosen facet (note that this type of projection is typical for humans' perception), which is known as *Schlegel diagram* [18]. However, the wire-frame projections show an information loss, and their comprehensibility decreases with the increase of complexity. Adding, e.g., colouring or gray scale shading to a 2D wire-frame image improves the content of information by one dimension [15]. Two or more 2D-images or the knowledge of regularity or symmetries of the depicted object help to read and interpret the image(s), i.e., to reconstruct the object in 4-space.

Another type of projection used for visual representation of polychora is based on the representation of a set of cells (solids) connected to each other along edges and vertices. Examples of such representation are described in [21, 14]. In the case of a relatively simple geometry, such projections can be more informative than the wire-frame ones. However, when the geometric complexity is quite high, there is an information loss caused by parts of objects (e.g., cells) which are out of the current view, e.g., the interior and the backside parts of an object. For increasing the informativity of such projections, several additional techniques were used for rendering. A significant increase of informativity can be obtained by using lighting and transparency together with the above-mentioned tools; this is often used for presenting higher-dimensional geometry [15].

There are many subtypes of 3D projections of higher-dimensional data and objects. One of the most often used is a representation of the higher-dimensional object as a set of colored 3D slices obtained during cutting the 4D object by hyperplanes with a defined step size. Sequences of 3D slices are often composed and animated, which improves the understanding of the geometry. Such approach finds an application in the visualization of higher-dimensional data in many scientific areas, mostly in physics [16] and medicine [7]. Results in this field are collected in [24], where the authors also describe an algorithm based on a sequence of 3D-slices, depicted one after the other as a sort of a movie, thus using the time scale as an additional dimension for the visualization process.

A specific method of projection for 4D polytopes onto a 3D space has been proposed by Boole Stott [3], an amateur mathematician, who rediscovered six four-dimensional regular convex polytopes and visualized them as 3D sections and unfoldings in 3D space [20]. Based on this approach, the on-line *Polyvise* tool for visualizing four-dimensional polytopes was developed [15]. This software uses some additional tools, e.g., coloring, transparency, emphasizing the edges and distortion of cells of a polytope for better comprehensibility.

When the initial iterations of higher-dimensional deterministic fractals are to be visualized, there is an additional problem caused by the very high complexity of the presented shapes. Since proper fractals cannot be visualized due to the infinitely many iterations, which should be performed on an initial object, usually a few initial iterations of such a fractal are displayed. The complexity of a deterministic fractal can be considered as the complexity of the contraction law (the law according to which the subsequent iterations of a fractal are constructed); this law can easily be figured out when looking at the figure(s). Depending on the complexity and other geometric parameters of a given iteration of a fractal, the projection type should be chosen appropriately.

Some advances in this area have been made in recent years. The first attempts in such higher-dimensional visualizations were made by Brisson [5]. In his work he presented a method of rendering the Sierpiński triangle, generalized to nD space and showed wire-frame-type projections. Frame and Neger [8] presented and discussed the Sierpiński hypertetrahedron (4D generalization of the Sierpiński triangle) in various orthogonal projections onto a

3D space, also as wire-frame-type projections.

The main goal of the presented work is to discover various types of projections of 4D deterministic fractals for finding the best looking and most informative ones with respect to their complexity. The projections were made for fractals based on the six regular convex polychora, which vary in geometric properties and complexity. Several approaches to render these fractals were presented, and some geometric aspects of the projections were also discussed.

2. Regular convex polychora and related fractals

The regular convex polychora (or 4D polytopes) are the 4D analogs of 3D regular convex polyhedra known as Platonic solids. There exist five such polyhedra in the 3D Euclidean space: tetrahedron, hexahedron, octahedron, dodecahedron, and icosahedron. These polyhedra can be generalized to the 4D Euclidean space and have the following names:

– the *pentatope* (analog of the tetrahedron),

– the *hypercube* (analog of the hexahedron),

– the *orthoplex* (analog of the octahedron),

– the *octaplex*,

– the *dodecaplex* (analog of the dodecahedron),

– and the *tetraplex* (analog of the icosahedron).

These regular convex polychora can be defined as subsets of the 4D space bounded by congruent Platonic solids, which are called the cells of the polychora.

– The pentatope consists of five regular teatrahedral cells, three of them meeting at each vertex.

– The hypercube consists of 8 cubic cells and 16 vertices, four cells meeting at each vertex.

– At the orthoplex there are 8 vertices, which connect 16 octahedral cells.

– The octaplex consists of 24 octahedral cells, 6 of them meet at each of the 24 vertices.

– The dodecaplex is composed of 120 dodecahedral cells, where at each of 600 vertices four cells are meeting.

– The tetraplex consists of 600 tetrahedral cells, 20 of them meet at each of the 120 vertices.

All of the above-presented polychora have 3D analogs except the octaplex, which has no direct analog in any other dimension [6]. Sometimes, the polychora are named according to the number of their 3D cells; e.g., the pentatope is also called 5-cell, the dodecaplex is called 120-cell, etc.

Since the above-presented polychora are regular (i.e., each of them has congruent regular faces and cells which are characterized by transitive symmetry), it is possible to construct related fractals by applying rules which are similar to those for the construction of fractals in the 3D space. Considering that there is no strict definition of a fractal, it is necessary to give the characteristic for deterministic fractals, which will be discussed here explicitly. Deterministic fractals can be constructed using the *Iterated Function Systems (IFS) algorithm* described in [13] for the 3D cases as follows.

Let A_0^P be a polychoron with a set of vertices v_n of A_0^P with coordinates $v_{n,m}$ ($m = 1,2,3,4$), in the Euclidean space $\mathbb{R}^4$, where P denotes a polychoron. The subscript of A denotes the number of contraction mapping iterations. Thus, the fractal based on a given polychoron is defined as the attractor A_∞^P of IFS, which is the set of

$$A_\infty^P = \bigcap_{i=0}^{\infty} h_i\left(A_0^P\right), \tag{1}$$

where $h_i()$ is an elementary similarity transformation.
The contraction process from A_k to A_{k+1}, $k \geq 0$, is realized using the Hutchinson operator:

$$H\left(A_\infty^P\right) = \bigcup_{i=1}^{N_k} h_i\left(A_k^P\right), \tag{2}$$

where N_k is a number of subsets for the k-th iteration, thus

$$\forall_{v_n \in A_k^P}\ h_i\left(v_n\right) = \frac{v_n}{r(P)} - \frac{v_i\left(1 - r(P)\right)}{r(P)}, \tag{3}$$

where $r(P)$ is the contraction ratio of a polychoron P, which ensures that the contractions of h_i are non-overlapped and non-disjointed: $h_i\left(A_k^P\right) \cap h_j\left(A_k^P\right) = \emptyset$, $i \neq j$. Such an object is the fractal in $\mathbb{R}^4$ of A_0^P with contraction ratio $r(P)$.

The contractions obtained by the above-described algorithm, scaled by the contraction ratio and placed inside the initial polychoron in such a way that every contraction has a common area with the initial polytope, constitute the first iteration of the fractal. In order to determine the next iteration, the same algorithm is applied for the contractions of the first iteration, etc. This ensures the hierarchical structure and infinite self-similarity of the considered fractal.

According to previous studies [10, 12], not all 4D-polytopes allow constructions of fractals in the way as mentioned above. However one can construct a Cantor-dust-like fractal by relaxing the above-presented conditions (the disjointed contractions). The Cantor-dust-like fractals are not of interest of this paper. The ability of construction depends on geometric and symmetry properties of the initial polychoron. In a previous study [11] it was proved that all regular convex polychora enable the construction of related fractals. Based on the construction presented above and the algorithms described in [11], the contraction ratios for fractals based on regular convex polychora can be determined. Their values are as follows:

- for the pentatope-based fractal $r = 2$,
- for the hypercube $r = 3$,
- for the orthoplex $r = 2$,
- for the octaplex $r = 3$,
- for the dodecaplex $r = 1 + \phi^2\sqrt{8}$, and
- for tetraplex $r = 1 + 2\phi$, where $\phi = \left(\sqrt{5} + 1\right)/2$ is the golden ratio.

Having the contraction ratios, it is possible to determine all coordinates of the contractions at the given iteration for any regular polychoron-based fractal. The values of the fractal dimensions corresponding to the mentioned fractals can be found in [11].

3. Projections of polychora-based fractals

Considering the fact that humans' perception is not adapted for visualizing 4D objects, the specific types of projections of these objects onto 3D space were developed, analogously to the well-known projections of 3D objects onto a plane. A review of projections from 4D to 3D for various coordinate systems can be found in [25].

Generally, there are two types of projections: parallel and perspective ones. Parallel projections preserve the dimensions of the visualized object without any distance distortions, e.g., the object looks the same at any distance from the observer. All of the projected points are projected directly to the lower-dimensional space. In the perspective projection the visualized object is scaled with respect to the distance from the observer. The objects become smaller with increasing distance from the observer, which is more suitable for the humans' perception. This is because the perspective projection is performed from a single point — the center of the projection, which is the same as if an observer looks at the object.

Taking into account that 4D objects with a very complex geometric structure are presented, it seems appropriate to use a perspective projection to visualize them. During the first step one needs to define two parameters: the distance d from the observer, which is a scalar value, and the direction of a projection $\vec{a} = (a_1, a_2, a_3, a_4)$, which is a 4D vector. The 4D perspective projection $p_i \in \mathbb{R}^4$ of a given point $v_i \in \mathbb{R}^4$ following the presented algorithm is as follows:

$$p_i = g\left(v_i + da_i\right), \tag{4}$$

where

$$g = \frac{d\sum_{i=1}^{4} a_i^2}{\sum_{i=1}^{4} a_i\left(v_i + da_i\right)}. \tag{5}$$

Then, in order to project the obtained 4D perspective onto 3D, the following expression is used:

$$t(x,y,z) = \frac{1}{l}\begin{pmatrix} a_4p_1 + a_3p_2 - a_2p_3 - a_1p_4 \\ -a_3p_1 + a_4p_2 + a_1p_3 - a_2p_4 \\ a_2p_1 - a_1p_2 + a_4p_3 - a_3p_4 \end{pmatrix} \quad \text{with} \quad l = \sqrt{\sum_{i=1}^{4} a_i^2} \tag{6}$$

as the normalization factor. Finally, in order to present a 3D projection as a 2D image, an orthogonal or perspective projection can be used (see, e.g., [19]).

There are four types of perspective projections applied most often to 4D polytopes: *vertex-first*, *edge-first*, *face-first*, and *cell-first* (see, e.g., [23]), which, in general can be represented by the vector

$$\mathbf{X} = x_1\vec{a}_1 + x_2\vec{a}_2 + x_3\vec{a}_3 + x_4\vec{a}_4, \tag{7}$$

where x_i are the coordinates of a general point and $\vec{a}$ is a basis. The names of projection types define the element toward which a given projection is oriented, e.g., in a vertex-first projection one of the vertices of a polychoron is the nearest to the 4D viewpoint. These types of projections are related to the 4D viewpoints defined by the direction vector $\vec{a}$:
for the vertex-first projection $\vec{a} = (1,1,1,0)$, for the edge-first $\vec{a} = (1,0,0,0)$, for the face-first $\vec{a} = (1,1,0,0)$ and for the cell-first $\vec{a} = (0,1,0,0)$.
However, such names have no strict definition and the elements of $\vec{a}$ could be slightly different from object to object [1]. Depending on the type of the chosen projection, the informativity of the rendered object varies. However, this is not a single problem. As it was mentioned above, there is another important criterion which influences the informativity of a given projection type. Depending on specific geometric properties and the complexity of an object, a given projection type can be very informative for one object, but poorly informative for another one. The notion of the informativity depends on an subjective evaluation of the observer, thus it is difficult to define it in a strict manner. However, the properties of the informativity are decribed in the following discussion of the investigated fractals.

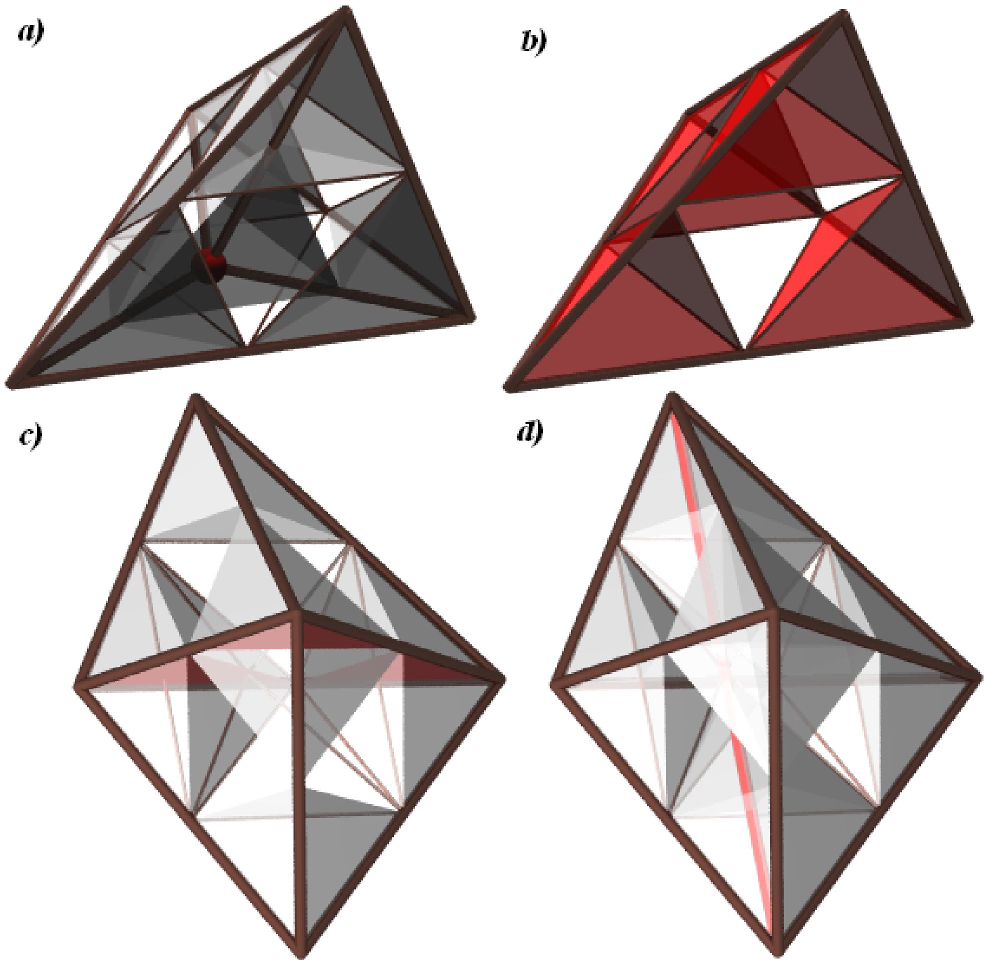

Figure 1: 2D visualizations of 3D perspective projections of the first iteration of a pentatope-based fractal: a) vertex-first, b) cell-first, c) face-first, d) edge-first.

Let us analyze and compare pentatope-based and hypercube-based fractals in the light of different types of perspective projections applied to them. The fractals in the first iteration are rendered with POV-Ray and presented in different projections in Figures 1 and 2. The fractals are rendered using some supporting tools, e.g., coloring and thickening of edges and cells and transparency of faces, what significantly improves the understanding of the geometry of the fractals. The contractions, which were projected at first, were highlighted by red color in the presented renders.

As it will be explained below, for the pentatope-based fractal the most informative and pleasant view is a vertex-first projection, while for the hypercube-based fractal a cell-first projection ist most suitable. This fact confirms that there is not only one right projection type for visualizing 4D deterministic fractals and other 4D objects. In order to describe the degree of informativity, one can use several concepts related to the psychology and humans' perception and cognition. Using the cognitive reference point, the approach described by the authors of [4] can explain why one perspective view seems to be more or less informative than the other.

Having the fundamental knowledge about 3D and 4D polytopes and their shapes, the observer expects similar shapes of the related fractals. Therefore, looking at the vertex-first projection of the first iteration of a pentatope-based fractal (Figure 1a) one can observe both

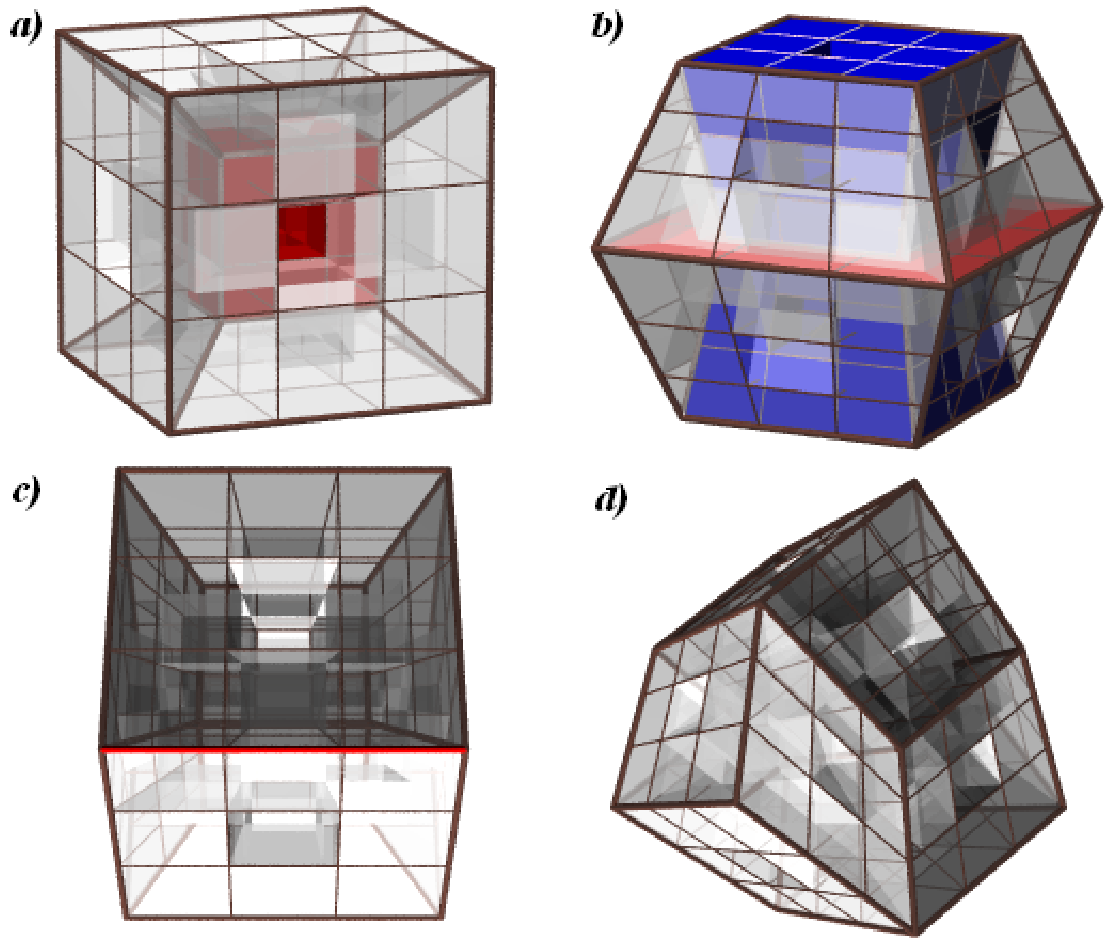

Figure 2: 2D visualizations of 3D perspective projections of the first iteration of a hypercube-based fractal: a) cell-first, b) face-first, c) edge-first, d) vertex-first.

4D dimensionality and self-similarity of the fractal. In the other projections presented in Figure 1 the self-similarity is well observable, but the dimensionality recognition is improper (without context one could conclude that the objects presented in Figure 1b, c, d are three-dimensional, especially the cell-first projection of the first iteration of a pentatope-based fractal — Figure 1b).

Similarly, in the case of hypercube-based fractal (Figure 2), considering the knowledge that the hypercube consists of 8 cubic cells, the observer expects that the fractal based on this polytope would look similar to the original polytope. Considering the presented projections, the cell-first (Figure 2a) and face-first (Figure 2b) projections of the first iteration of a hypercube-based fractal fulfill the criteria of visibility of 4D dimensionality and fractal self-similarity, and can be considered as projections with a high degree of informativity, while in the case of the two latter projections none of these criteria is fulfilled.

The visualizations described above are suitable for 4D fractals, which are characterized by a low degree of complexity. In the case of orthoplex-based and octaplex-based fractals, the same technique makes the rendered image unclear, resulting in numerous intersections and stratification of transparent faces. In such cases it is more appropriate to visualize a wire-frame projection with a single filled cell, which is more informative than visualizing the cells of a whole fractal. An exemplary cell-first projection of orthoplex-based fractal is presented

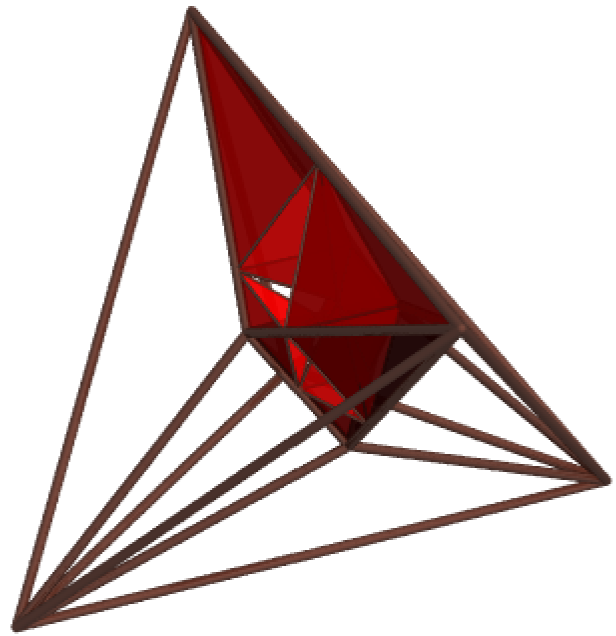

Figure 3: 2D visualization of a 3D cell-first perspective projection of the first iteration of an orthoplex-based fractal with one filled cell.

in Figure 3.

In the case of 4D fractals with a very complex geometric structure, the above-presented methods can be inefficient, because they consist of a lot of edges and faces, which intersect and stratify each other. After iterating the fractals, the number of edges and faces increases rapidly and makes the image completely incomprehensible. Therefore, it is necessary to apply some other projection types for visualizing the fractals. A great way to visualize high-dimensional structures with high degree of complexity is to distort the cells that form a given polychoron, a technique proposed by Boole Stott [3]. The perspective projections described above present a polytope or a polytope-based fractal in the form of a subset in $\mathbb{R}^4$ bounded by congruent polyhedra of $\mathbb{R}^3$. The main idea behind Boole Stott's technique, which she used to calculate 3D sections of polychora, is first folding out these polychora onto the 3D space using 3D perpendicular and diagonal sections [3].

This approach could be successfully adapted for the visualization of a tetraplex-based fractal. In order to increase the informativity of projection, the different colors were assigned to the particular sections. The resulted vertex-first projection of tetraplex-based fractal is presented in Figure 4.

For visualizing the dodecaplex-based fractal, a specific topologic representation is used. The geometric structure of the dodecaplex makes it possible to visualize it as a discrete Hopf fibration, which allows to present this polychoron as a set of 12 rings, which are intertwined with each other in a spiral manner. This Hopf-type visualization method is also applicable to other polytopes. Mathematically, the Hopf fibration could be considered as a two-step projection of an object [22]. Firstly, the radial projection $\mathbb{R}^4 \setminus \{0\} \to \mathrm{S}^3 \subset \mathbb{R}^4$ is applied, which results in the transformation of $v_i \in \mathbb{R}^4$ as follows:

$$v_i\,(w,x,y,z) \mapsto \frac{(w,x,y,z)}{|(w,x,y,z)|}. \tag{8}$$

Then follows the stereographic projection $\mathrm{S}^3 \setminus \{N\} \to \mathbb{R}^3$, which results in the transformation

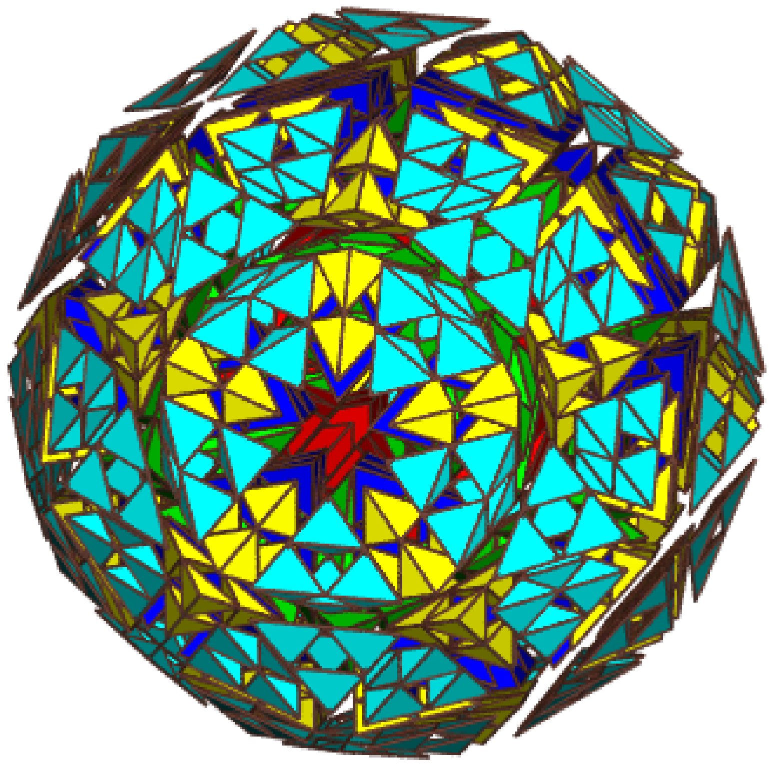

Figure 4: 2D visualization of a 3D vertex-first perspective projection of the first iteration of a tetraplex-based fractal with distorted cells.

of $\tilde{v}_i \in \mathrm{S}^3$ as below:

$$\tilde{v}_i\,(w, x, y, z) \mapsto \left(\frac{x}{1-w}, \frac{y}{1-w}, \frac{z}{1-w}\right). \tag{9}$$

Using this approach, the dodecaplex-based fractal (as well as hypercube- and octaplex-based fractals) can be presented. In Figure 5 two and five rings, respectively, are presented. In the visualizations each dodecahedral cell consists of 20 dodecahedral contractions of the first iteration of a fractal, distorted for more clear representation.

4. Conclusions

This paper presented various methods and projection types for visualizing higher-dimensional deterministic fractals. The geometric complexity of such objects requires advanced visualization tools and algebraic transformations in order to achieve the most pleasant looking and the most informative projections of 4D fractals. The analysis of visual representation of 4D fractals was made basing on regular convex polychora-based fractals. As it was shown in Figures 1 and 2, there is no single suitable projection for all investigated fractals. The comprehensibility of a structure of a given fractal depends on several parameters, mainly on the geometric complexity and the choice of an appropriate projection.

In the case of fractals with a low degree of complexity, the projection type has crucial significance, because it is connected with a quantity of lost information during the projection from 4D to 3D. An additional aspect, which may have a significant influence on the information loss, is the use of rendering tools, i.e., coloring, thickening and transparency of the presented higher-dimensional objects.

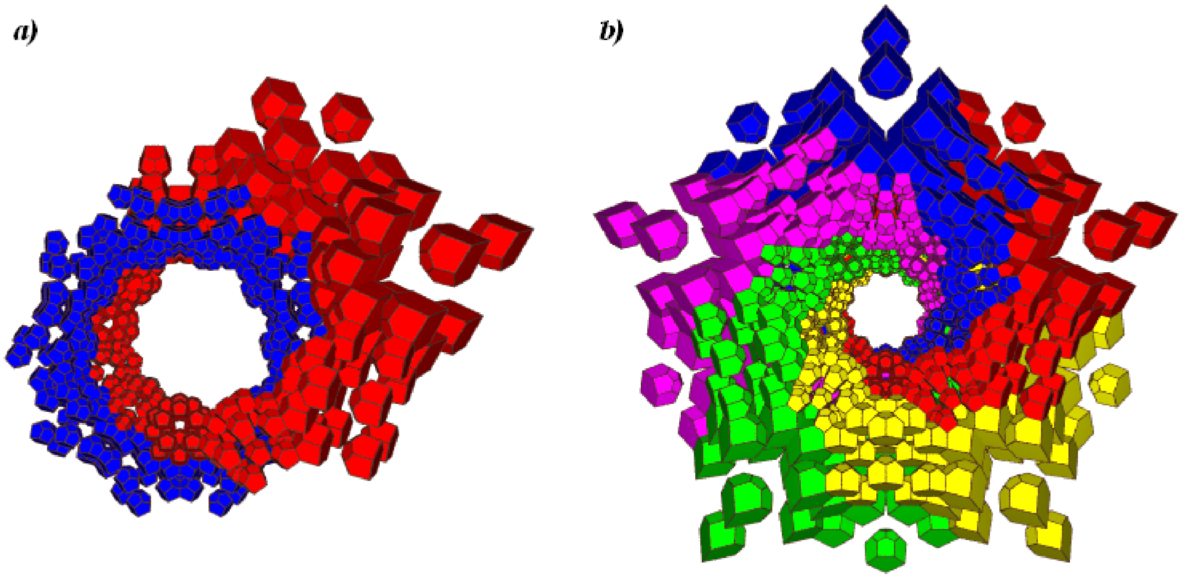

Figure 5: 2D visualizations of the first iteration fo a dodecaplex-based fractal as a discrete Hopf fibration: a) two rings of fibration, b) five rings of fibration.

In the case of 4D fractals with a high degree of complexity, the projection type is not so significant, and the usage of rendering tools decreases the comprehensibility of a presented object. The problem of their visualization could be solved using the unfolding technique proposed by Boole Stott and a Hopf fibration. These techniques offer a possibility to visualize an internal structure of 3D projections of 4D objects. This application was presented for the two most complex fractals, namely the dodecaplex- and the tetraplex- based ones. The presented visualization techniques may be used as guidelines for visualizing the fractals investigated in this paper as well as other 4D deterministic fractals.

References

[1] J. Barnes: *Gems of Geometry*. Springer, Berlin-Heidelberg 2012.

[2] J. Bokowski, J.-P. Roudneff, T.-K. Strempel: *Cell decompositions of the projective plane with Petrie polygons of constant length*. Discrete Comput. Geom. **17**, 377–392 (1997).

[3] A. Boole Stott: *On certain series of sections of the regular four-dimensional hypersolids*. Verh. Konink. Akad. **7**, 1–21 (1900).

[4] B.F. Bowdle, D. Gentner: *Informativity and assymetry in comparisons*. Cognitive Psychol. **34**, 244–286 (1997).

[5] G.F. Brisson: *Sierpinski fractals from words in high dimensions*. Chaos Soliton. Fract. **5**, 2191–2200 (1995).

[6] H.S.M. Coxeter: *Regular Polytopes*. Courier Dover Publications, Toronto 1973.

[7] A.W. Dowsey, J. Keegan, M. Lerotic, S. Thom, D. Firmin, G.-Z. Yang: *Motion-compensated MR valve imaging with COMB tag tracking and super-resolution enhancement*. Med. Image Anal. **11**, 478–491 (2007).

[8] M. Frame, N. Neger: *Fractal tetrahedra: What's left in, what's left out, and how to build one in four dimensions*. Comput. Graph. **32**, 371–381 (2008).

[9] A.J. Hanson, P.A. Heng: *Visualizing the fourth dimension using geometry and light*. Proc. of IEEE Conf. Visualization '91, San Diego 1991, pp. 321–328.

[10] A. Katunin: *Deterministic fractals based on Archimedean solids*. Sci. Res. Inst. Math. Comput. Sc. **10**, 93–100 (2011).

[11] A. Katunin: *Fractals based on regular convex polytopes*. Sci. Res. Inst. Math. Comput. Sci. **11**, 53–62 (2012).

[12] A. Katunin, D. Kurzyk: *General rules of fractals construction from polyhedra*. J. Geometry Graphics **16**, 129–137 (2012).

[13] A. Kunnen, S. Schlicker: *Regular Sierpinski polyhedra*. Pi Mu Epsilon J. **10**, 607–619 (1998).

[14] E. Molnár, J. Katona, I. Prok, J. Szirmai: *The regular 120-cell in 4-space and it's visualization*. Proc. 4th Internat. Scientific Conference on Geometry and Graphics, moNGeometrija, Vlasina/Serbia 2014, pp. 214–215.

[15] J. Morey, K. Sedig: *Adjusting degree of visual complexity: an interactive approach for exploring four-dimensional polytopes*. Visual Comput. **20**, 565–585 (2004).

[16] M. Morháč, V. Matoušek: *Interactive visualization of multidimensional coincidence spectra*. PMC Physics A **1**, 1–36 (2007).

[17] A.M Noll: *A computer technique for displaying n-dimensional hyperobjects*. Commun. ACM **10**, 469–473 (1967).

[18] A. Pacheco, P. Real: *Getting topological information for a 80-adjacency doxel-based 4D volume through a polytopal cell complex*. Lecture Notes Comput. Sci. **5856**, 279–286 (2009).

[19] Z. Pizlo: *3D Shape: Its Unique Place in Visual Perception*. MIT Press, Cambridge/MA 2010.

[20] I. Polo-Blanco, J. Gonzalez-Sanchez: *Four-dimensional polytopes: Alicia Boole Stott's algorithm*. Math. Intell. **32**, 1–6 (2010).

[21] I. Prok: `http://www.math.bme.hu/~prok`. Accessed Mar 26, 2015.

[22] S. Schleimer, H. Segerman: *Puzzling the 120-cell*. ArXiv.org, 2013, `http://arxiv.org/abs/1310.3549`. Accessed Mar 26, 2015.

[23] C.H. Séquin: *Symmetrical projections of the high-dimensional regular polytopes*. Symmetry **11**, 65–84 (2000).

[24] J. Woodring, H.-W. Shen: *Chronovolumes: a direct rendering technique for visualizing time-varying data*. Proc. VG03, 3rd Internat. Workshop on Volume Graphics, Tokyo 2003, pp. 27–34.

[25] S. Zachariáš, D. Velichová: *Projection from 4D to 3D*. J. Geometry Graphics **4**, 55–69 (2000).

Received September 14, 2014; final form March 26, 2015